

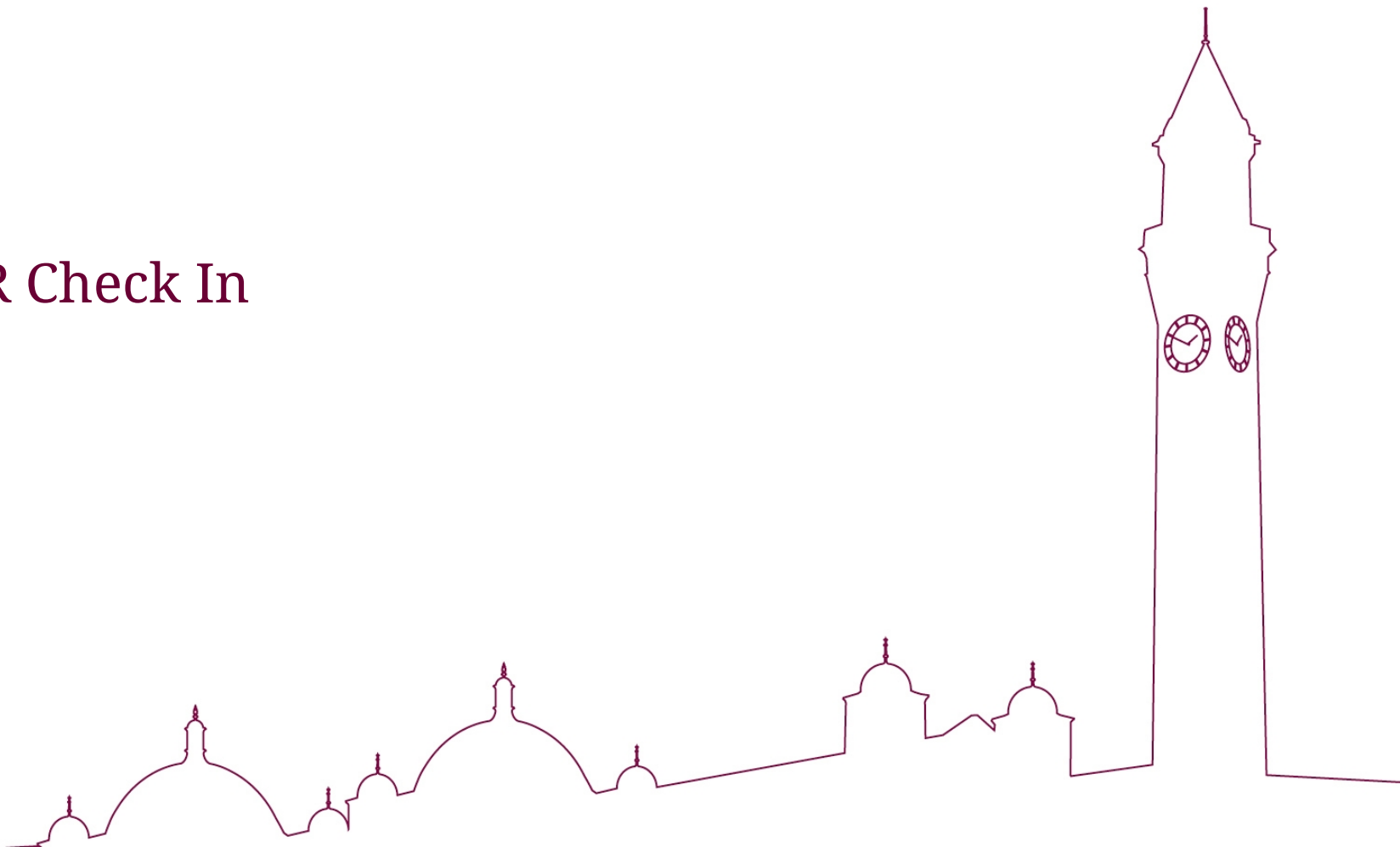


UNIVERSITY OF  
BIRMINGHAM

SCHOOL OF  
PHYSICS AND  
ASTRONOMY

# Inclusive ESR Check In

S. Maple, W. Lin



# Overview

- Appendix A.1: DIS electron selection
  - Short section to refer to where required → Done?
- Appendix A.2 NC ep reduced cross sections
  - Text written, just needs cleaning up. Replace fig. 9 with March campaign, update uncertainties in fig. 10
- Appendix A.3-4 Proton  $F_2$  and  $F_L$  structure functions and PDFs
  - Text written, needs cleaning up + references re-adding
- Appendix A.5  $F_2$  ratio in e+Au
  - Text written, needs cleaning up, maybe some extra info, and references.
- Appendix A.6 Double spin asymmetry and spin dependent structure functions
  - Text written, figures need updating to March campaign and some style changes

# A.2

- Update figures to March campaign
- Minor text updates

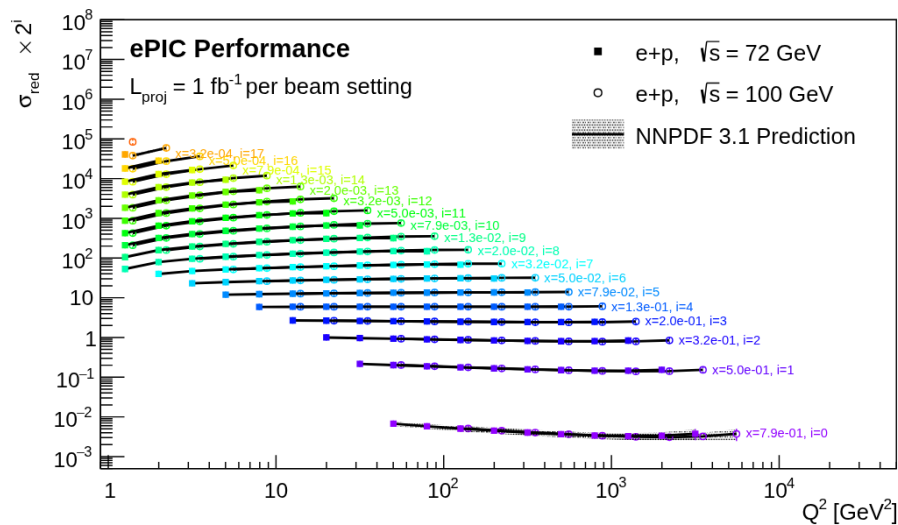


Figure 10: Cross sections and uncertainties for the 10x130 and 10x250 GeV<sup>2</sup> ep beam configuration as a function of  $Q^2$  with no purity/stability requirement. Points are offset in  $Q^2$  for visibility. The uncertainties are taken as the sum in quadrature of the statistical uncertainty and a 3.9 % total systematic uncertainty. **SM update figure - smaller errors needed.**

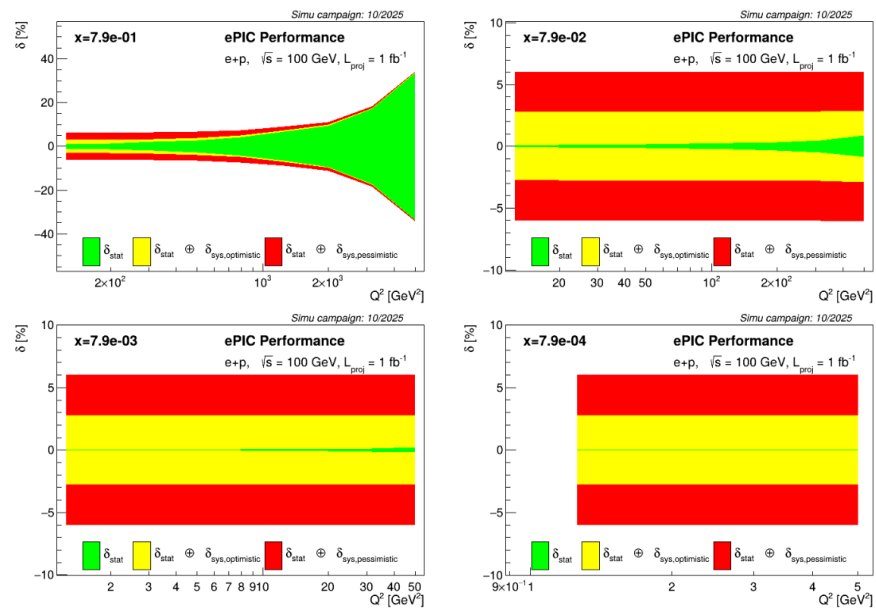


Figure 9: Cross section uncertainties for the 10x250 GeV<sup>2</sup> ep beam configuration as a function of  $Q^2$  at four values of  $x$  **SM update figure.**

# A.3

## Mainly text updates

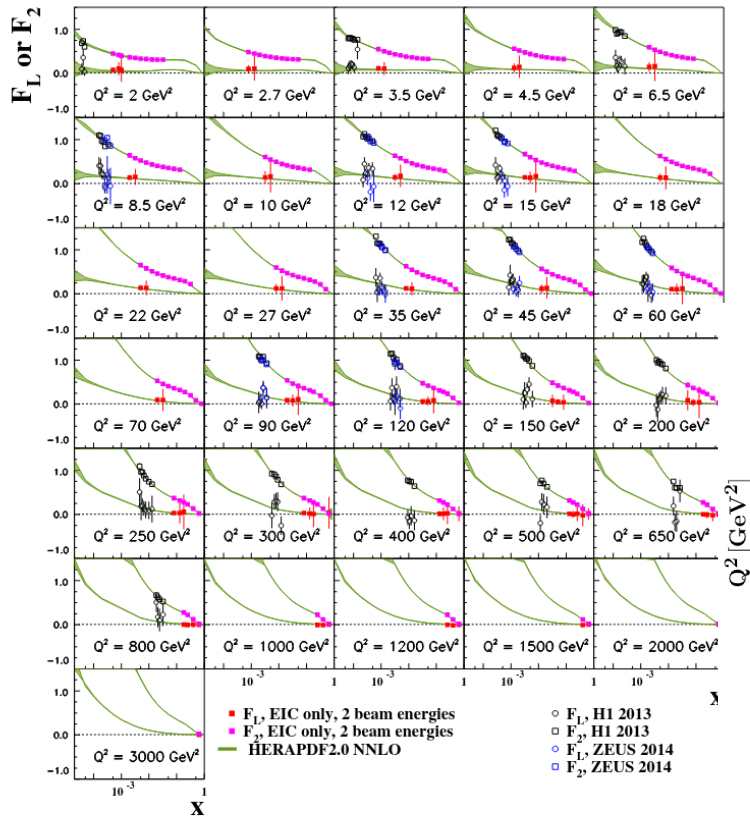


Figure 11: Simulated extractions of  $F_2$  and  $F_L$  for fits with the two standard EIC early science beam energy configurations of  $\sqrt{s} = 100$  and 72 GeV. The error bars on the points represent the total experimental uncertainties. For the  $F_L$  measurements, points with absolute uncertainties larger than 0.5 are removed for visual clarity but all points for the corresponding  $F_2$  measurements are shown.

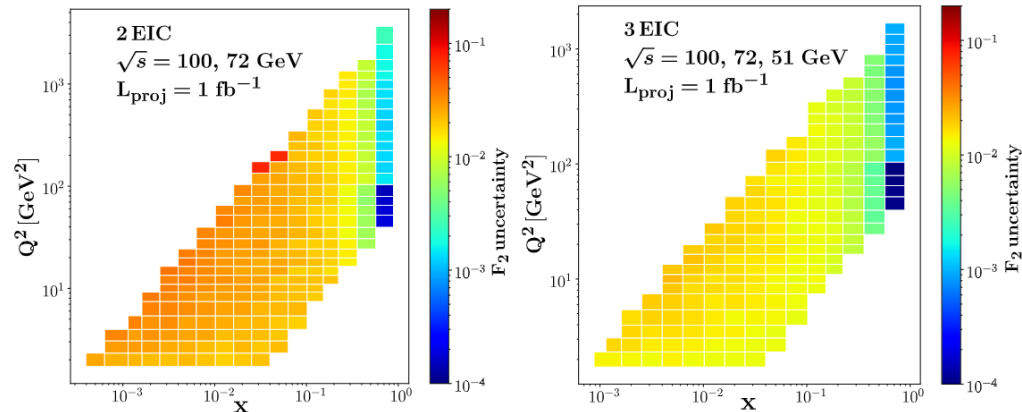


Figure 14: Absolute uncertainties on the simulated early science  $F_2$  measurements, corresponding to the two (left) and three (right) beam energy configurations, with the colors indicating the absolute uncertainties.

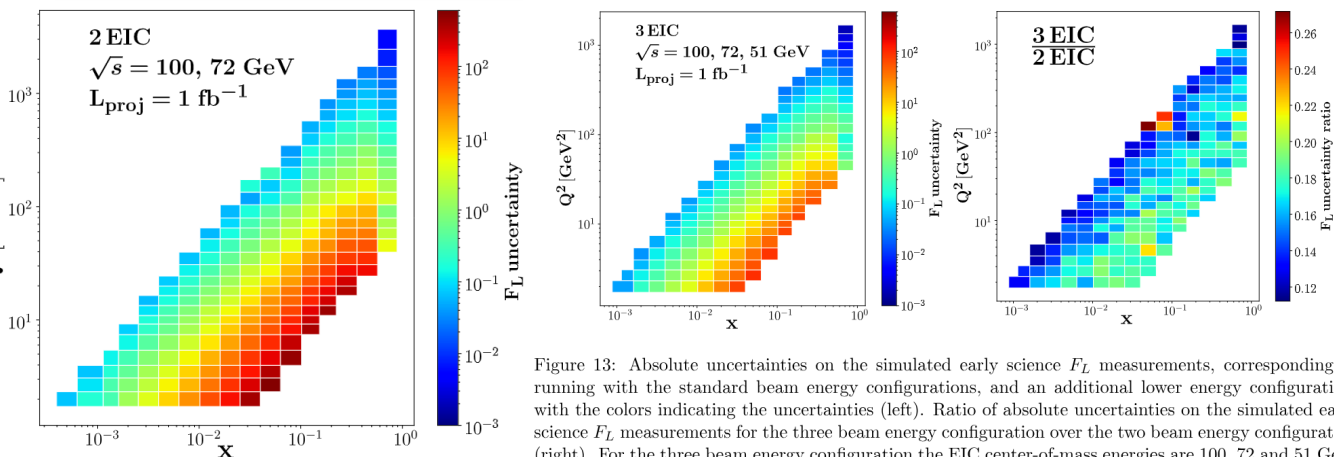


Figure 13: Absolute uncertainties on the simulated early science  $F_L$  measurements, corresponding to running with the standard beam energy configurations, and an additional lower energy configuration, with the colors indicating the uncertainties (left). Ratio of absolute uncertainties on the simulated early science  $F_L$  measurements for the three beam energy configuration over the two beam energy configuration (right). For the three beam energy configuration the EIC center-of-mass energies are 100, 72 and 51 GeV. For the two beam energy configuration the EIC center-of-mass energies are 100 and 72 GeV. Note that different methods are applied in the two cases, with all three beam energies required to be available in the Rosenbluth fits for the ‘3 EIC’ extraction and just two required for the ‘2 EIC’ case.

# A.4

- Mainly text updates

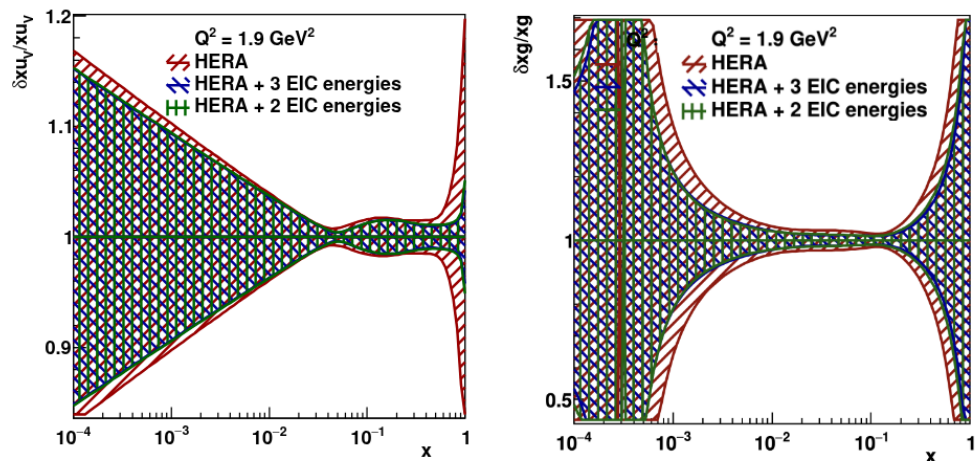


Figure 15: Impact of simulated EIC data on the NNLO collinear parton distributions of the proton, shown on a logarithmic  $x$  scale. The bands show relative experimental uncertainties for the up-valence and gluon distributions for  $Q^2 = 1.9 \text{ GeV}^2$ . The HERAPDF2.0NNLO total uncertainties are compared with results in which simulated EIC data for different beam energy scenarios are also included in the HERAPDF2.0NNLO fitting framework. Beam settings are  $\sqrt{s} = 100$  and  $72 \text{ GeV}$  for the two-beam case, with  $\sqrt{s} = 51 \text{ GeV}$  added for the three-beam case.

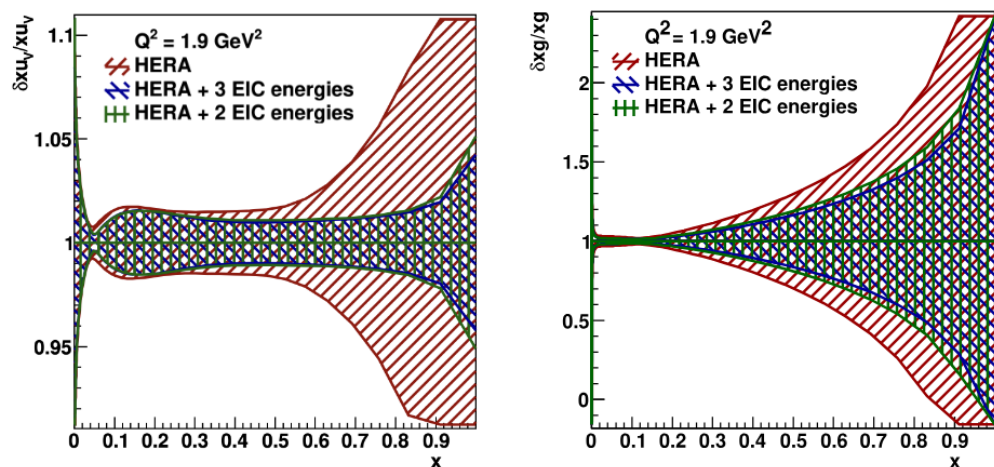


Figure 16: Impact of simulated EIC data on the NNLO collinear parton distributions of the proton, shown on a linear  $x$  scale. The bands show relative experimental uncertainties for the up-valence and gluon distributions for  $Q^2 = 1.9 \text{ GeV}^2$ . The HERAPDF2.0NNLO total uncertainties are compared with results in which simulated EIC data for different beam energy scenarios are also included in the HERAPDF2.0NNLO fitting framework. Beam settings are  $\sqrt{s} = 100$  and  $72 \text{ GeV}$  for the two-beam case, with  $\sqrt{s} = 51 \text{ GeV}$  added for the three-beam case.

# A.5

- Cleaning up text, minor additions, add references

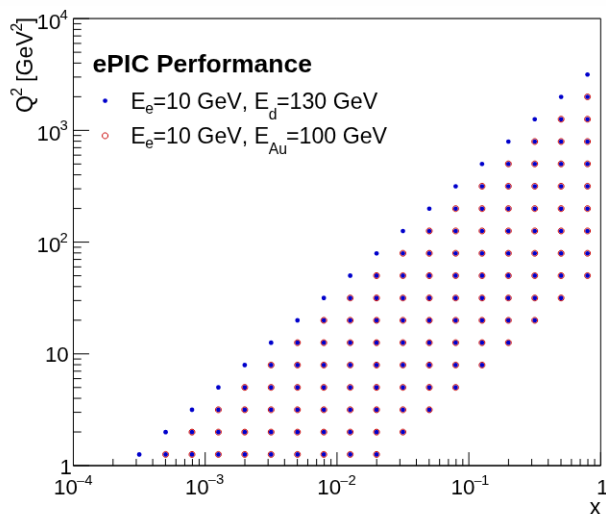


Figure 17: Kinematic coverage of inclusive cross section measurements for the EIC early science  $10 \times 130$  GeV<sup>2</sup>  $e + d$  and  $10 \times 100$  GeV<sup>2</sup>  $e + Au$  beam energy configurations, for five bins per decade in  $x$  and  $Q^2$ , with  $Q^2 > 1$  GeV<sup>2</sup> and  $0.01 < y < 0.95$ .

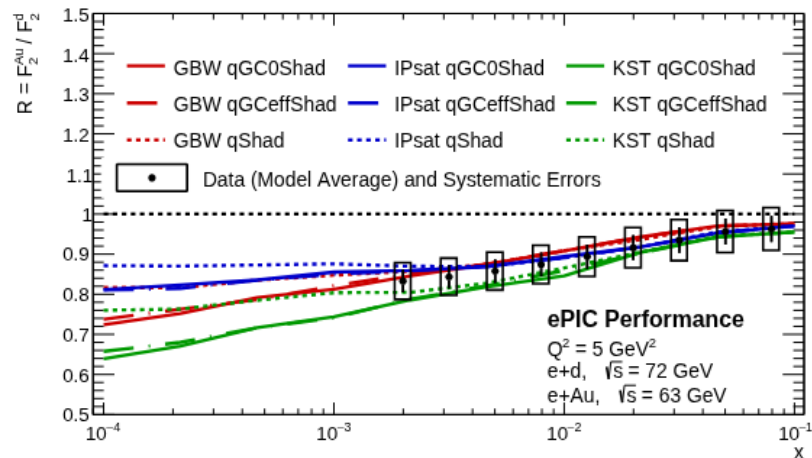
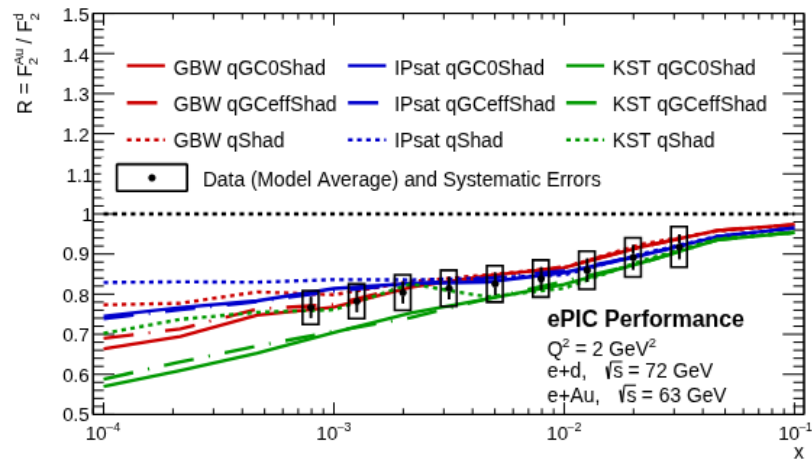


Figure 18: Projected measurements of the per-nucleon  $F_2$  structure function ratio for  $^{197}\text{Au}$  to the deuteron as a function of  $x$ , at  $Q^2 = 2$  GeV<sup>2</sup> (top) and  $Q^2 = 5$  GeV<sup>2</sup> (bottom). The error bars indicate an optimistic 3.4 % estimate for the total measurement uncertainty, and the boxes a pessimistic 5.5 % estimate. The points are overlaid on predictions from different phenomenological models of the dipole cross section (GBW, IPsat, KST), for calculations using only the lowest  $|q\bar{q}|$  component of the photon (qShad) and for two calculations using the higher Fock component of the photon containing gluons (qGC0Shad, qGCeffShad) [15]. The points are positioned at the average  $R$  value of the nine model predictions.



# A.6

- Figures to be updated w/ recent campaign and more readable text

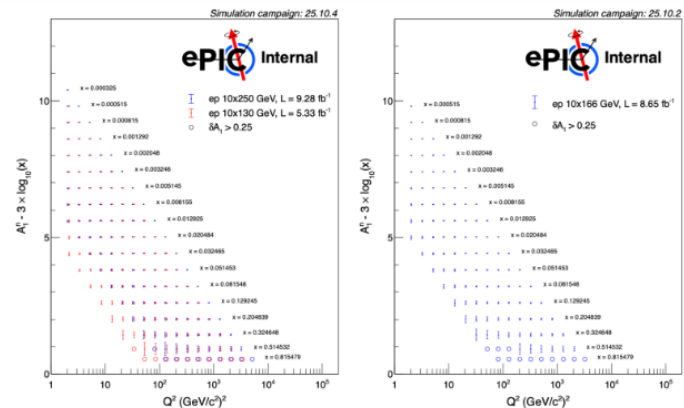


Figure 19: Projected measurements of  $A_1^0$  (left) and  $A_1^+$  (right) with estimated statistical uncertainty.

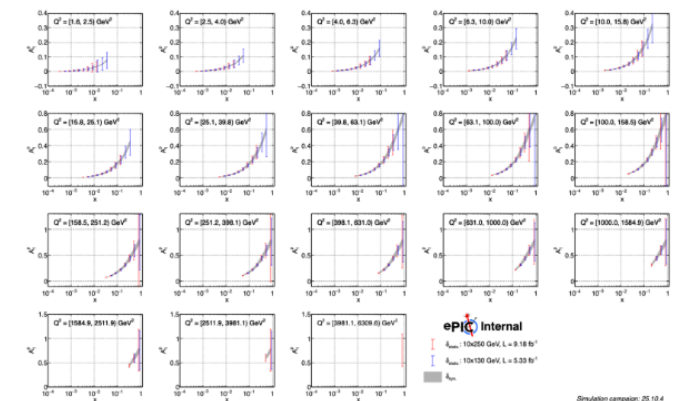


Figure 20: Projected measurements of  $A_1^0$  with estimated statistical and systematic uncertainties for each  $Q^2$  bin. (Will make figure text bigger)

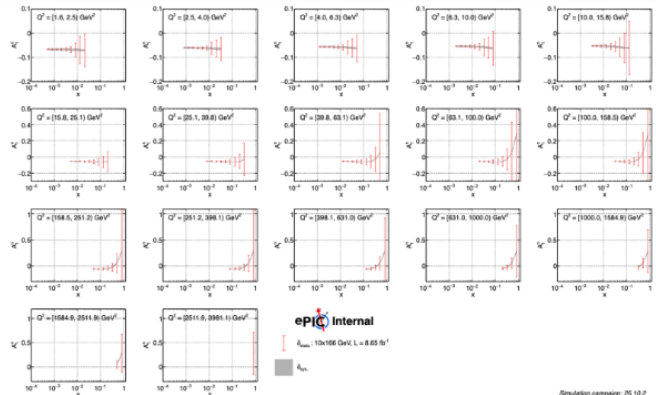


Figure 21: Projected measurements of  $A_1^+$  with estimated statistical and systematic uncertainties for each  $Q^2$  bin. (Will make figure text bigger)

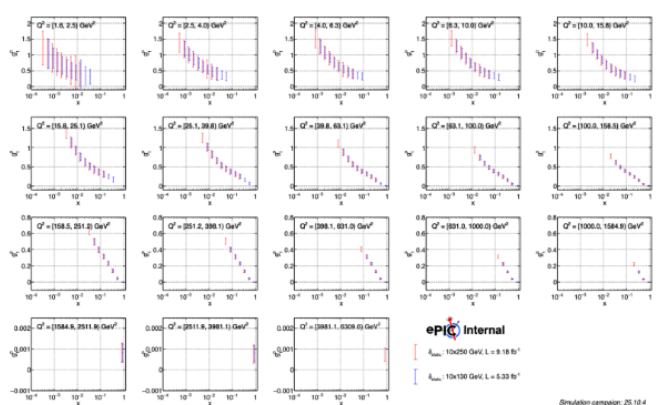


Figure 22: Projected measurements of  $g_1^0$  with estimated statistical uncertainties for each  $Q^2$  bin. (Will make figure text bigger)

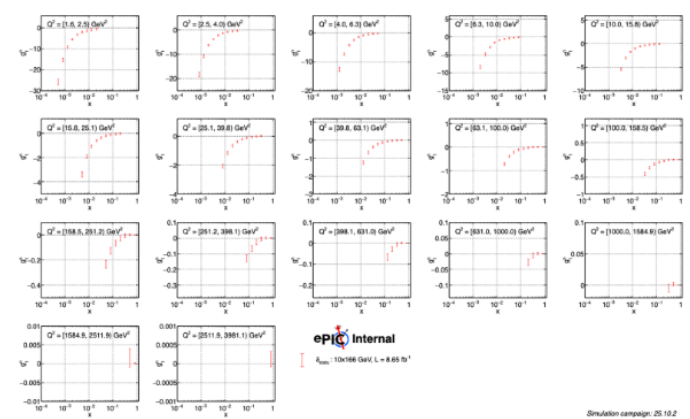


Figure 23: Projected measurements of  $g_1^+$  with estimated statistical uncertainties for each  $Q^2$  bin. (Will make figure text bigger)

